DESIGN STUDY OF AN IHX SUPPORT STRUCTURE FOR A POOL-TYPE SODIUM-COOLED FAST REACTOR

CHANG-GYU PARK*, JONG-BUM KIM and JAE-HAN LEE
Korea Atomic Energy Research Institute
1045 Daedeokdaero, Yuseong-gu, Daejeon, 305-353, Korea
*Corresponding author. E-mail : chgpark@kaeri.re.kr

The IHX (Intermediate Heat eXchanger) for a pool-type SFR (Sodium-cooled Fast Reactor) system transfers heat from the primary high temperature sodium to the intermediate cold temperature sodium. The upper structure of the IHX is a co-axial structure designed to form a flow path for both the secondary high temperature and low temperature sodium. The co-axial structure of the IHX consists of a central downcomer and riser for the incoming and outgoing intermediate sodium, respectively. The IHX of a pool-type SFR is supported at the upper surface of the reactor head with an IHX support structure that connects the IHX riser cylinder to the reactor head. The reactor head is generally maintained at the low temperature regime, but the riser cylinder is exposed in the elevated temperature region. The resultant complicated temperature distribution of the co-axial structure including the IHX support structure may induce a severe thermal stress distribution. In this study, the structural feasibility of the current upper support structure concept is investigated through a preliminary stress analysis and an alternative design concept to accommodate the IHTS (Intermediate Heat Transport System) piping expansion loads and severe thermal stress is proposed. Through the structural analysis it is found that the alternative design concept is effective in reducing the thermal stress and acquiring structural integrity.

1. INTRODUCTION

The SFR (Sodium-cooled Fast Reactor) system adopts an IHTS (Intermediate Heat Transport System) to prevent contact of the irradiated primary sodium from the SWR (Sodium-Water Reaction) with the SG (Steam Generator) feed water. The IHTS transfers reactor-generated heat from the PHTS (Primary Heat Transport System) to the steam generator system and it is composed of an IHX (Intermediate Heat eXchanger), the SG, a secondary coolant circulation pump, and piping connecting each component. For a pool-type SFR system, the IHX, which transfers the heat from the primary radioactive sodium to the intermediate non-radioactive sodium, is submerged into the primary sodium pool in the RV (Reactor Vessel) and is supported on the RH (Reactor Head).

The IHX generally used in a SFR system consists of upper and lower tubesheets separated by a heat transfer tube, with a central downcomer and a riser for incoming and outgoing intermediate sodium, respectively[1]. In particular, the upper part of the IHX adopts a co-axial structure, thus creating a multi-layered cylindrical structure. Most of the IHXs in the pool-type SFR system inevitably adopt a co-axial structure type IHX upper part to realize a compact component arrangement. The co-axial structure creates concurrent flow paths of the incoming and outgoing intermediate sodium through the inside and outside cylinder structure without necessitating other structures.

A large capacity SFR system requires a large diametric piping for a 2-loop IHTS layout. Since a large diameter piping induces severe thermal loads, the IHX co-axial structure, to which the IHTS piping is connected, is regarded as a critical structural component due to the IHTS piping connection and severe thermal load conditions. Moreover, the IHX support structure is exposed to a wide temperature region, ranging from elevated temperature above 500 °C to low temperature of about 200 °C, and thus a severe thermal gradient arises in the compact IHX support structure.

In this paper, the structural features of a co-axial IHX upper part are investigated and the stress intensity is compared with that yielded by an alternative design model. From the comparison study, an adequate alternative co-axial design concept for a pool type SFR system is proposed and its structural integrity against a representative cycle event is evaluated according to the ASME Code rules for a specified cycle event.

2. DESIGN FEATURES OF IHX SUPPORT STRUCTURE

Figure 1 shows a schematic drawing of the co-axial structure of the IHX upper part. This structure is applied in PRISM (Power Reactor Inherently Safe Module), the conceptual design of a 1245MWe liquid metal reactor electric generating power station studied by General Electric Company. PRISM uses nine reactor modules and each module produces 425MW of thermal power[1].

As shown in Fig. 1, a central downcomer cylinder guides the cold intermediate sodium to the IHX lower plenum and the hot intermediate sodium enters the IHTS piping through the annular space outside the downcomer cylinder. The IHX support is welded into the outer cylinder of the annular space and it is located on the RH, which is normally maintained at a relatively low temperature.

The IHX co-axial structure is composed of 4 layers, the downcomer, intermediate cylinder, IHX riser, and IHX support, as shown in Fig. 1. The intermediate cylinder is installed to prevent direct contact of the hot and cold sodium at both sides of the downcomer and thus the radial thermal stress of the downcomer can be reduced. The thermal loss of the intermediate cylinder toward the downcomer is minimized by installing thermal insulation between the downcomer and the intermediate cylinder. Thermal insulation and guard piping are installed outside of the co-axial structure to prevent heat loss and sodium leak toward the RH.

KALIMER-600[2,3], which is a Korea Advanced

Liquid Metal Reactor of a pool-type with a 600MWe capacity and sodium coolant, adopts an upper skirt type support structure for the IHX similar to the PRISM support structure. The support structure outside the IHX riser undertakes the primary compression loading due to the IHX dead weight. The heat loss of the IHX riser to the support structure and RH is prevented by applying insulation between the IHX riser and the support structure.

The reactor system under consideration in this paper adopts a 2-loop IHTS with a 60 year lifetime and the IHTS piping connected to the co-axial piping is assumed to have a 90.0cm diameter. The IHX and IHTS piping will be constructed from 9Cr-1Mo-V steel and thus dissimilar welding between each component can be excluded. The support structure and riser are assumed to have 6.75cm and 6.5cm thickness, respectively; these values were obtained after carrying out several preliminary structural analyses. The reactor head supporting the IHX has a 50.0cm thickness. It is assumed that an expansion bellows is applied at the upper part of the downcomer to accommodate the axial thermal expansion difference between the IHX tubes and downcomer. Therefore, the co-axial structure is assumed to be free from an axial thermal expansion constraint caused by the downcomer and the intermediate cylinder.

3. PRELIMINARY STRUCTURAL FEASIBILITY

3.1 Primary Loads

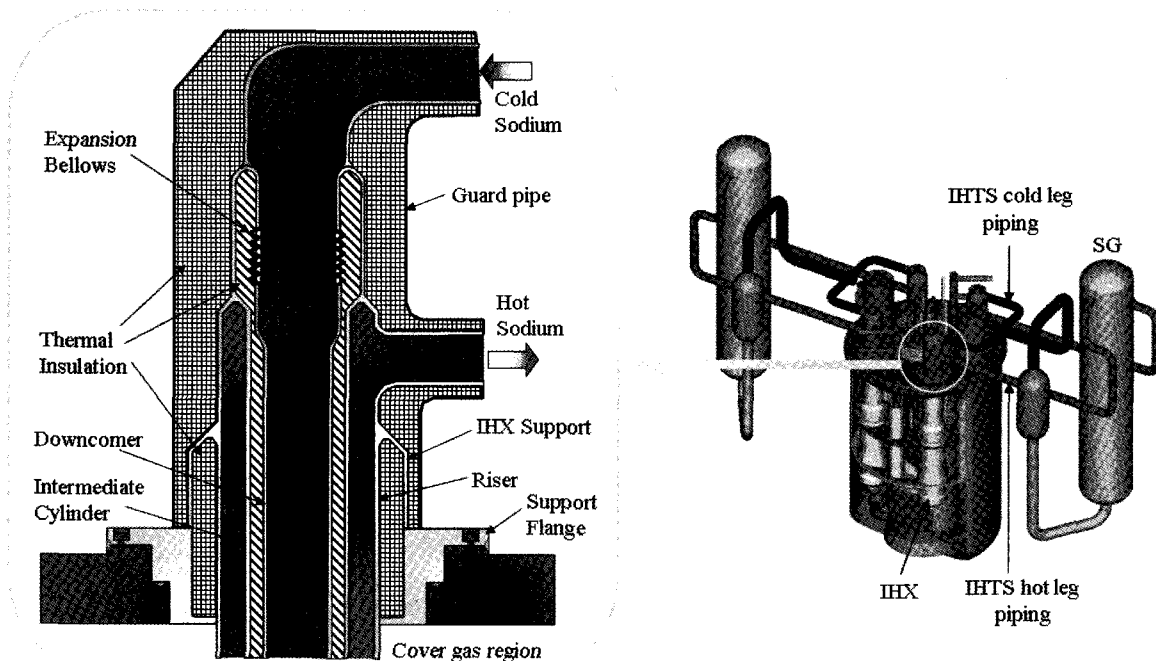The structure dead weight and the IHTS piping expansion

Fig. 1. Schematic Conceptual Drawing of the Upper Support Type IHX Co-axial Structure

loads are considered as representative primary loads. The weight of the IHX is conservatively assumed to be 80 tons, and it is uniformly applied to the IHX riser. The IHTS cold leg is assumed to accommodate the axial thermal expansion through the piping layout because of its low temperature condition, and thus the thermal expansion load by the IHTS cold leg is not included with the primary loads. However, the IHTS hot leg is supported at the co-axial structure and steam generator, and this constraint functions as a primary load on the co-axial piping.

The piping thermal expansion load can be calculated by performing a piping stress analysis. In this paper, the finite element analysis program used for the piping analysis is ANSYS[4] software and it provides the PIPING Element as well as 3-D Element for the piping model analysis. Figures 2(a) and 2(b) show the reaction results of the IHTS hot leg piping obtained using the PIPING Element model and a 3-D Element model at the steady state condition, respectively. As shown in Fig. 2, the PIPING Element model induces more conservative reaction results than
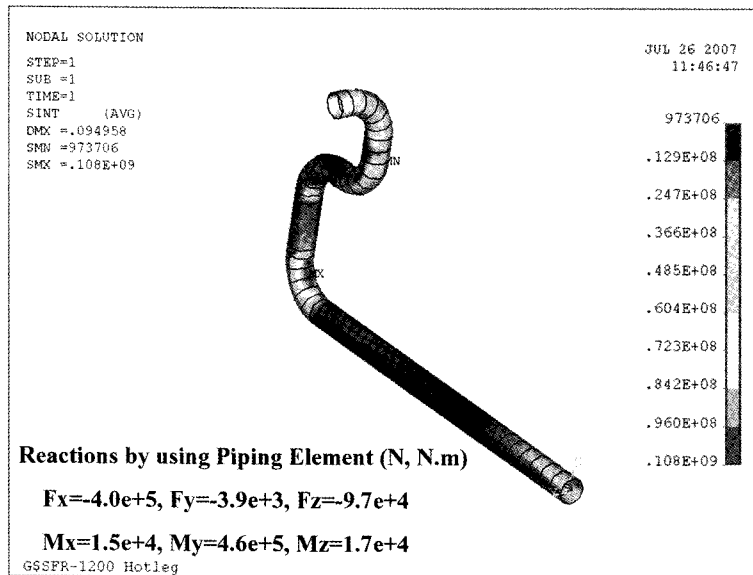
(a) Reactions by using PIPING Element.
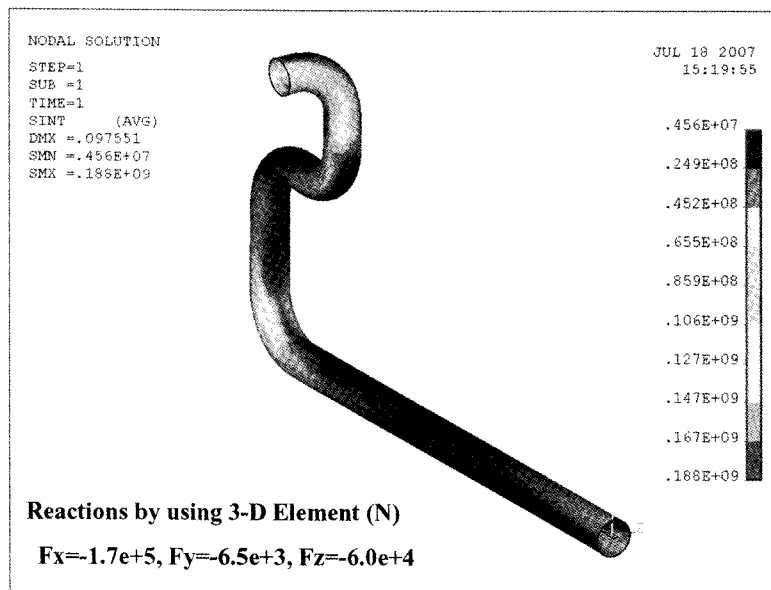
(b) Reactions by using 3-D Element.

Fig. 2. Reaction Results of the IHTS Hot Leg Piping According to the Element Types

those obtained using the 3-D Element model. Therefore, the reaction results obtained using the PIPING Element are selected as the primary loads that act upon the co-axial structure. From Fig.2(a) and Fig.2(b), it appears that there is a large difference in the maximum stress value of the two models. However, this is caused only by the inherent features of employed elements, not by any difference in the boundary conditions. The piping element only provides the sectional stress value while the 3-D element model gives the specified nodal position such as the elbow outer surface. For Fig. 2, the sectional average stress value around the maximum stress node of the 3-D model is 101MPa, a value that is very close to the piping element result, i.e., 108MPa. The temperature-dependent material properties are utilized based on ASME Section II, Part D[5] and Section III, Subsection NH except for the density and specific heat, which are selected from RCC-MR Section I, Subsection Z[6].

With the calculated load conditions, a half-symmetric analysis model with a 3-dimensional solid finite element is constructed and a preliminary stress analysis is carried out to judge the feasibility of the structural design concept for the primary loading condition. The element types used in the analysis are SOLID70 for a thermal analysis and SOLID45 for a stress analysis, provided by the ANSYS program. The maximum stress intensity occurs in the junction part of the IHTS hot leg and the riser cylinder, as shown in Figure 3. The maximum stress intensity section is exposed at the elevated temperature region (at about 528 °C) at the steady state condition, and thus the stress limits are evaluated by Subsection NH[7] Code rules. The primary stress limits for a Level A service are as follows:

$$P_m \leq S_{mt} \tag{1}$$

$$P_L + P_b \leq KS_m \tag{2}$$

$$P_L + P_b / K_t \leq S_t \tag{3}$$

where P_m is the general primary membrane stress intensity, and P_L and P_b denote the local primary membrane stress components and the primary bending stress components. S_{mt} is the allowable limit of the general primary membrane stress intensity, S_m is the lowest stress intensity value at a given temperature among the time-independent strength quantities, and S_t is a temperature and time-dependent stress intensity limit.

Figure 3 shows that the maximum stress intensity value including the membrane, bending, and peak stresses is about 50MPa. Considering that S_{mt} and S_m at 525 °C and a 300,000 hold time condition provided in Subsection NH Code are 106MPa[7], it is found that the evaluation model of Fig. 3 satisfies the primary stress limits with sufficient margins.

3.2 Thermal Loads

Class 1 components have to be evaluated according to the ASME Section III Subsection NH procedure for the elevated temperature region and Subsection NB[8] procedure for the low temperature region. Therefore, the structural integrity of the co-axial structure under thermal loads has to be evaluated by considering the temperature distribution results. The following are the assumed heat transfer conditions used to carry out the thermal analysis:

- The outer surface of the co-axial structure is thermally insulated.
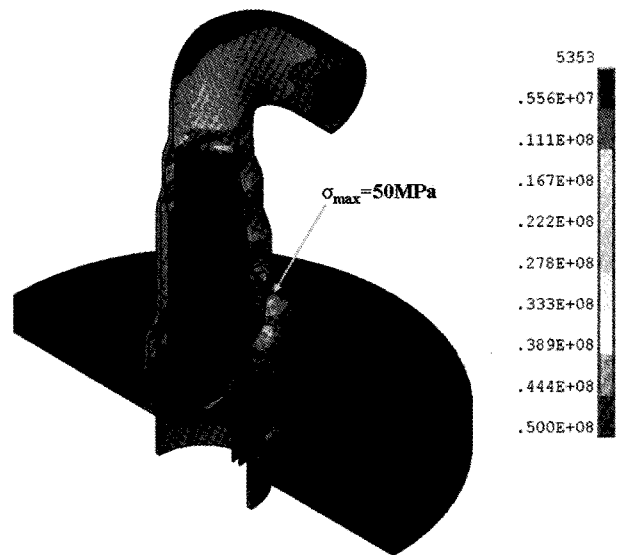

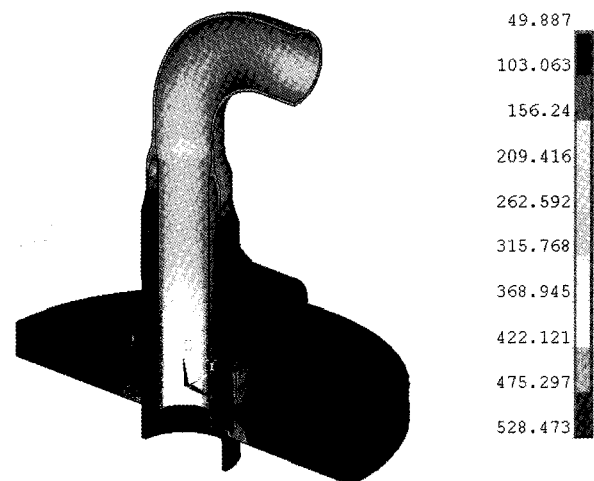Fig. 3. Primary Stress Intensity Distribution of the Upper Support Type Co-axial Structure

Fig. 4. Temperature Distribution of the Upper Support Type co-Axial Structure at Steady State Condition

- The inner surface temperature of the cylinder containing a coolant is equal to the coolant temperature.
- Heat convection by air cooling with 40 °C, 90W/m²·K is assumed on the RH upper surface to maintain the maximum temperature of the RH under the 150 °C region[3].
- The IHX support structure and the insulation support structure that supports the insulation material and protects the cover-gas in RV from leakage toward the RH exterior are welded into the RH and IHX riser, respectively.

Figure 4 shows the heat transfer analysis results at the normal operating full power condition. Since the outer surface of the structure is assumed to be thermally insulated, the structural temperature is almost same as the coolant temperature. However, the IHX support structure and insulation support structure show a steep temperature gradient and thus it causes a severe thermal stress intensity, as shown in Fig. 5. The maximum stress intensity occurs at the insulation support structure between the IHX riser and RH with 2,000MPa. Therefore, the RH of the current design concept should not be welded into the IHX riser directly, because the radial thermal expansion difference between the IHX riser and RH induces severe thermal stress on the junction part. Additionally, the IHX support structure undergoes a steep temperature gradient, leading to a thermal stress intensity of approximately 450MPa. Although a long IHX support structure is likely to release the longitudinal thermal gradient of the support structure, it is vulnerable to momentum forces stemming from the piping thermal expansion, and thus the height of the co-axial structure should be designed with this aspect taken into consideration. Therefore, it is judged that the current design concept is not adequate for a pool-type SFR with
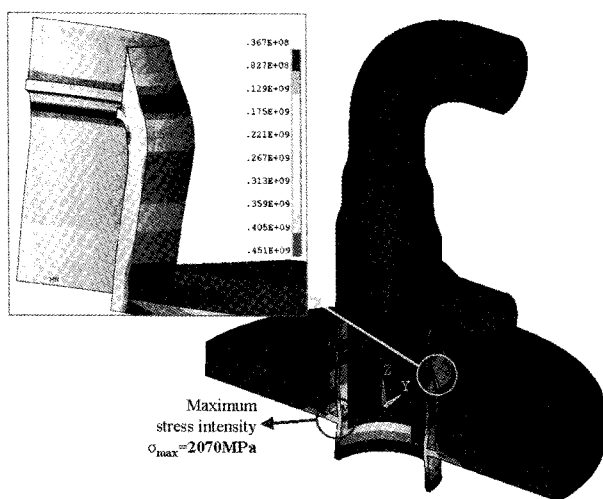
an elevated temperature operating condition, and thus an alternative design concept for a co-axial structure should be proposed.

4. ALTERNATIVE DESIGN CONCEPT

Since the KALIMER has an elevated temperature operating condition and large diametric IHTS piping in comparison with the PRISM, implementation of an upper skirt type support structure for the KALIMER is less economical and is not feasible without changing the height of the co-axial structure. An alternative design concept of the IHX support is required for the KALIMER system, because changing the height of the co-axial structure may affect the system performance as well as IHX performance, although the magnitude would not be severe.

4.1 Structural Features

The structural weakness of Fig. 1's concept is caused by the structural constraints for the thermal expansion and thermal gradient. The thermal gradient can be released by lengthening the object model under the same thermal boundary. The current IHX has a riser cylinder of 4.5m from the RH upper surface to the IHX upper plenum. The

Fig. 5. Thermal Stress Intensity Result of the Upper Support Type Co-axial Structure at Steady State Condition
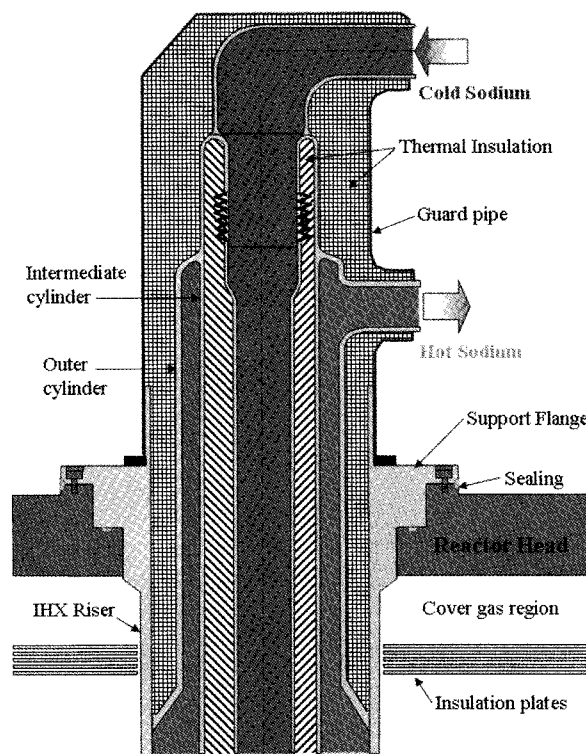

Fig. 6. Schematic Drawing of an Alternative Design Concept Using the Lower Support Type Structure

alternative design concept is to extend the IHX outer shell to the RH and the extended shell functions as the IHX riser. Figure 6 presents a schematic drawing of the alternative design concept, referred to as the lower support type in this paper. Several design concepts to reduce the stress compared with the original model were studied and the alternative design concept was selected through consideration of the stress level as well as manufacturability, fabricability, and accessibility for inspection. The IHX riser supports the IHX on the RH, and the outer cylinder between the IHX riser and intermediate cylinder is welded into the hot leg piping to guide the hot sodium without heat loss to the IHX riser. This model allows easy installation of the thermal insulation between the IHX riser and outer cylinder. In addition, in contrast with the upper support type, the lower support type effectively releases the thermal gradient of the support structure without necessitating a height change of the co-axial structure, and thus it is possible to eliminate the superfluous height between the reactor head and the hot leg piping. It also has similar structural features to the upper skirt type structure in terms of manufacturing, handling, and inspection. Furthermore, the IHX performance is not affected by the support structure type, because there is no change to the dimensions or geometries of the coolant guide cylinders.

4.2 Temperature Distribution

To evaluate the structural integrity of the alternative

concept according to the ASME Codes, its temperature distribution has to be calculated first. Figure 7 shows the temperature distribution of the alternative model at normal operating conditions. The temperature of the cylindrical structure guiding the coolant flow path is the same as the coolant temperature, but the IHX riser has a variable temperature distribution, from 528 °C to 200 °C. Thus, this temperature distribution causes thermal stress in the IHX riser.

4.3 Load Controlled Stress Limits

The primary load and boundary conditions of the alternative model are the same as those of the upper support model. To evaluate the structural integrity of the alternative model according to the ASME procedure, a primary stress analysis is carried out, as shown in Fig. 8. From the primary loading analysis, two critical sections are selected, as shown in Fig. 8. The selected sections are the structural discontinuity parts of the hot leg piping nozzle (Section-1) and y-junction structure (Section-2) between the outer cylinder and the IHX riser. Since these sections are exposed to an elevated temperature of about 528 °C as shown in Fig. 7, their structural integrity is evaluated according to the ASME Subsection NH procedure in this paper.

The design limits for the load controlled stress of the Level A Service are described in Eqs.(1)~(3). For Section-1, the stress intensity values of the primary membrane and the primary membrane plus bending are 17.7MPa


```
ANSYS 10.0
NODAL SOLUTION
STEP=1
SUB =1
TIME=1
TEMP      (AVG)
RSYS=0
PowerGraphics
EFACET=1
AVRES=Mat
SMN =44.3
SMX =528.003

XV  =.446298
YV  =-.758684
ZV  =.474571
*DIST=4.256
*XF  =.19791
*YF  =.413737
*ZF  =1.074
A-ZS=-51.201
Z-BUFFER
    44.3
    98.045
    151.789
    205.534
    259.279
    313.024
    366.769
    420.514
    474.259
    528.003
```
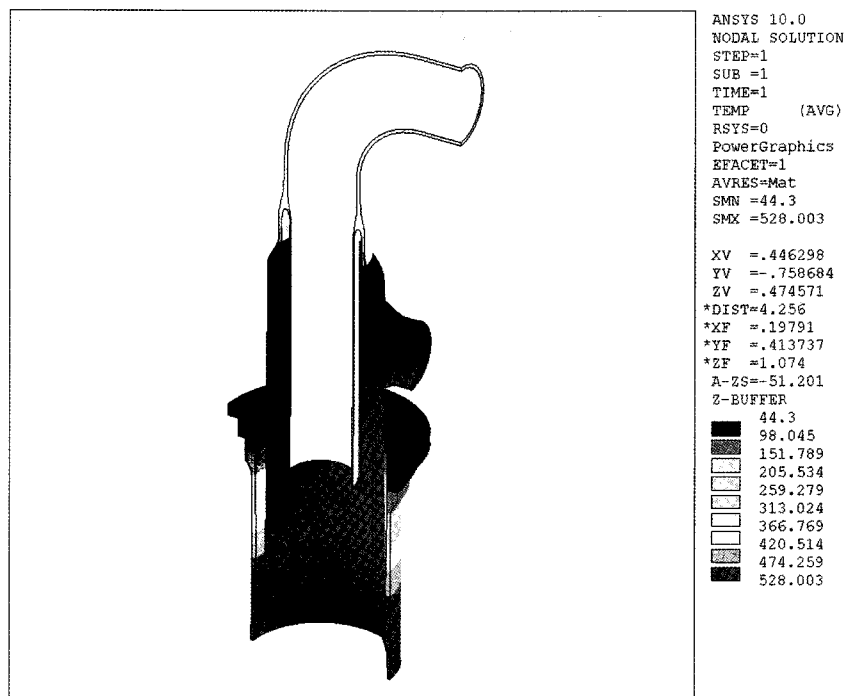
Fig. 7. Temperature Distribution of Alternative Model at Normal Operating Conditions

and 67.7MPa, and their design limit values are 94.6MPa and 202.5MPa, respectively. For Section-2, the stress intensity values of the primary membrane and the primary membrane plus bending are 24.6MPa and 52.1MPa, and their design limit values are 94.6MPa and 202.5MPa, respectively. The maximum use-fraction sums associated with the general primary membrane stress and the primary membrane plus bending stress by considering the 60 year lifetime satisfy the evaluation limits as follows:

$$\sum_i \left(\frac{t_i}{t_{im}} \right) = \frac{525,600h}{2,233,400h} = 0.24 \leq 1.0 \text{ for membrane stress}$$

$$\sum_i \left(\frac{t_i}{t_{imb}} \right) = \frac{525,600h}{1,360,800h} = 0.39 \leq 1.0 \text{ for membrane+bending stress}$$

(Section-1)

$$\sum_i \left(\frac{t_i}{t_{im}} \right) = \frac{525,600h}{2,077,800h} = 0.26 \leq 1.0 \text{ for membrane stress}$$

$$\sum_i \left(\frac{t_i}{t_{imb}} \right) = \frac{525,600h}{1,582,200h} = 0.34 \leq 1.0 \text{ for membrane+bending stress}$$

(Section-2)

where t_i is the design lifetime of 60 years and t_{im} and t_{imb}

are the maximum allowable times for the membrane stress and the membrane plus bending stress, respectively. From these results, the selected critical sections of alternative model satisfy the design limits for the load controlled stress.

4.4 Deformation Controlled Limits

ASME Subsection NH for Class 1 components in elevated temperature service requires the strains and deformation limits from specified operating conditions as well as the load controlled stress limits, and provides the Appendix T procedure to this end. While a complete list of the duty cycle events is necessary for a detailed structural integrity evaluation, the assumed transient event to evaluate the structural integrity in this paper is a refueling cycle event, which takes the temperature history from the refueling temperature (200 °C) to the normal operating temperature (528 °C). Figure 9 shows the stress intensity contour at the steady state condition. The maximum stress intensity value of the alternative model by a thermal load occurs at the IHX riser with 96.1MPa; this value is much smaller than that of the upper support structure model.

The employed design hold time is 500,000 hours. The assumed refueling interval is 1.5 years[3], and thus the number of cycle events for this lifetime is 40. However, in this paper, we conservatively assumed the number of cycle events to be 400, which includes a hot standby event that is assumed to occur every 2 months. The design and
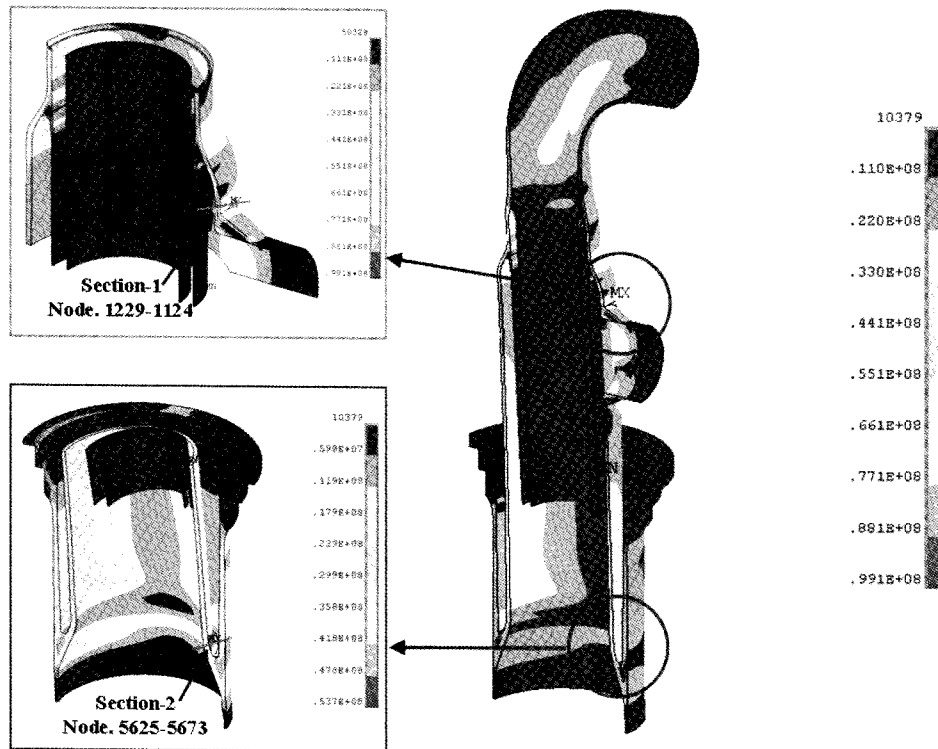

Fig. 8. Primary Stress Intensity Results of the Alternative Model and Selection of the Evaluation Sections

```
ANSYS 10.0
NODAL SOLUTION
STEP=1
SUB =1
TIME=1
SINT      (AVG)
PowerGraphics
EFACET=1
AVRES=Mat
DMX =.039104
SMN =315.362
SMX =.961E+08

XV  =.33326
YV  =-.859205
ZV  =.388207
*DIST=4.834
*XF  =.281808
*YF  =.516682
*ZF  =1.23
A-ZS=-44.888
Z-BUFFER
      315.362
      .107E+08
      .213E+08
      .320E+08
      .427E+08
      .534E+08
      .640E+08
      .747E+08
      .854E+08
      .961E+08
```
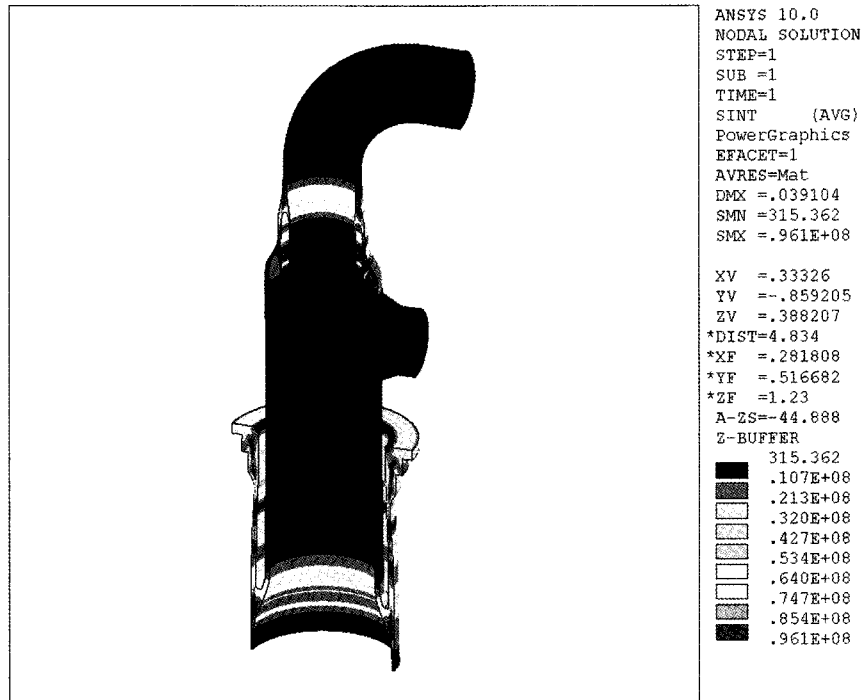
Fig. 9. Thermal Stress Intensity Contour of the Alternative Model
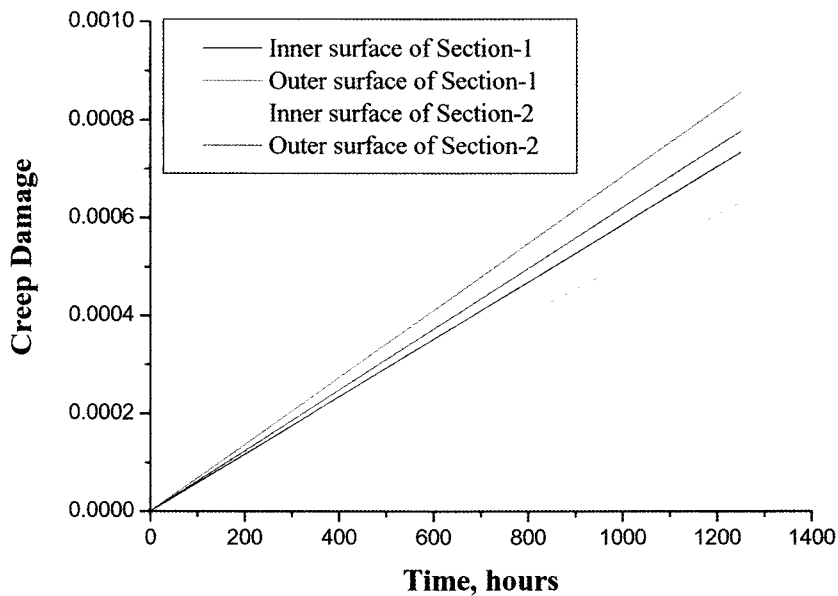

Fig. 10. Calculated Creep Damage Accumulation Time Histories of the Alternative Model for One Cycle

material values for a 500,000 hour lifetime are obtained by extrapolating the ASME Subsection NH data provided for a hold time of 300,000 hours.

Appendix T of Subsection NH is mainly composed of deformation and strain limits and a creep-fatigue damage evaluation. Strain limits are evaluated by using an elastic analysis approach and a simplified inelastic analysis

approach. The strain limits given by the elastic analysis approach require that the limit satisfy any one of the three test equations[9]. The calculated $X+Y$ values for Section-1 and Section-2 are 0.216 and 0.209, respectively, and they meet the design limit of 1.0 with a sufficient design margin. The creep-ratcheting strain values calculated by the simplified inelastic analysis approach for Section-1

Table 1. Summary of the Structural Integrity Evaluation Results

Evaluation Items		Section-1		Section-2	
		Calculated	Limits	Calculated	Limits
Primary stress limits(MPa)	Membrane	17.7	94.6	24.6	94.6
	Membrane+Bending	67.7	202.5	52.1	202.5
Deformation & strain limits	Elastic Approach	0.216	1.0	0.209	1.0
	Simplified Inelastic Approach(%)	0.051	1.0	0.032	1.0
Creep-Fatigue damage	Fatigue Damage	0.288e-6	0.066	0.287e-6	0.069
	Creep Damage	0.343	1.0	0.311	1.0

and Section-2 are 0.051% and 0.032%, respectively, while their limit value is 1.0%. This means that only slight creep ratcheting is expected for a given cycle event during the whole operating time.

The creep-fatigue damage must not exceed the creep-fatigue damage envelope diagram. For Section-1, the maximum elastic strain range (ε_{max}) obtained from the ANSYS analysis result is 0.010% and the modified strain range (ε_{mod}) calculated from ε_{max} is 0.012%. The total strain range (ε_t) is 0.013% and the allowable number of cycles(N_d) obtained by the total strain range is 1.39e+9 cycles. The strain values of ε_{max} and ε_t for Section-2 are 0.011% and 0.013%, respectively, and the allowable number of cycles is 1.39e+9 cycles. The fatigue damages for Section-1 and Section-2 are 0.288e-6 and 0.287e-6, respectively, meaning that the fatigue damage for both sections is almost negligible due to the small ε_t values. The creep damage of Section-1 and Section-2 for the whole operating time is 0.343 and 0.311, respectively, meeting the allowable creep damage of 1.0 calculated by considering the negligible fatigue damage. Figure 10 shows the calculated creep damage accumulation time histories for one cycle obtained using the SIE ASME-NH program[10], which provides a computerized implementation of the ASME Pressure Vessels and Piping Code Section III Subsection NH Code [11] and Table 1 presents a summary of the results of the structural integrity evaluation for both sections subjected to a given cycle event. The structural integrity is not evaluated here for the dynamic loads. However, we can speculate that the alternative design is more beneficial than the original design in this regard, because the original design has a greater height requirement for the co-axial structure than the alternative design, and thus the former will be more strongly affected by dynamic loads.

5. CONCLUSIONS

A pool-type SFR generally adopts a co-axial structure as an IHX upper structure connecting the IHTS piping and IHX component to accomplish a compact design of the

IHX. The structural features of the IHX upper support type were investigated first and a preliminary stress analysis for the structure was carried out. From the analysis results, it was found that the upper support type is not suitable for a reactor system where there is a large temperature difference between the IHTS hot sodium and the reactor head, and direct contact of the hot sodium cylinder of the IHX with the reactor head should be avoided. To accommodate the upper support structure concept to the elevated temperature SFR system, a co-axial structure with increased height is necessary; however, this change to the component height would detrimentally affect the system performance. Therefore, as an alternative design concept for the IHTS support, a lower support type was proposed. Despite having a similar structure, it readily releases the steep thermal gradient of the support structure between the hot sodium cylinder and reactor head. From an investigation of the design features and high temperature structural evaluations of the lower support structure, it was found that the proposed lower support concept is suitable in terms of releasing the effect of the thermal loads of the IHX support structure. Moreover, the lower support structure satisfies the ASME design limits of Level A Service with sufficient margins for a given representative elevated temperature cycle event by a conceptual analysis. It is, however, still necessary to comprehensively ensure the structural integrity of the IHX support structure for all duty cycle events.

ACKNOWLEDGEMENTS

REFERENCES

[1] *Modular Liquid Metal Reactor(LMR) Design Technology*, GE, USA (1992).
[2] Dohee Hahn, et al., KALIMER-600 Conceptual Design Report, KAERI/TR-3381/2007, Korea Atomic Energy Research Institute (2007).
[3] Dohee Hahn, Y. Kim, C. Lee, S. Kim, J. Lee, Y. Lee, B. Kim and H. Jeong, "Conceptual design of the Sodium-

Cooled Fast Reactor KALIMER-600," *Nuclear Engineering and Technology*, **39**, 3 (2007).

[4] ANSYS Release 10.0, ANSYS Inc (2005).

[5] *ASME Boiler and Pressure Vessel Code, Section II, Part D, Properties*, 2004 Edition, ASME (2004).

[6] *RCC-MR Design and Construction Rules for Mechanical Components of FBR Nuclear Islands, Section I-Subsection Z : Technical Appendix A3*, AFCEN (2002).

[7] *ASME Boiler and Pressure Vessel Code, Section III, Division 1 – Subsection NH*, 2004 Edition, ASME (2004).

[8] *ASME Boiler and Pressure Vessel Code, Section III, Division 1 – Subsection NB*, 2004 Edition, ASME (2004).

[9] G. H. Koo, Computer Program of SIE ASME-NH Code (Revision 1), KAERI/TR-3526/2008, Korea Atomic Energy Research Institute (2008).

[10] SIE ASME-NH, Structural Integrity Evaluation Program by the ASME Subsection NH code, Korea Atomic Energy Research Institute (2008).

[11] Gyeong-Hoi Koo and Jae-Han Lee, "Development of an ASME-NH program for nuclear component design at elevated temperatures," *International Journal of Pressure Vessels and Piping*, **85**, pp385-393 (2008).